


# Fabrication and Oxidation Resistance of TiAl Matrix Coatings Reinforced with Silicide Precipitates Produced by Heat Treatment of Warm Sprayed Coatings

Judyta Sienkiewicz<sup>1</sup>  · Seiji Kuroda<sup>2</sup> · Hideyuki Murakami<sup>2</sup> · Hiroshi Araki<sup>2</sup> · Maciej Giżyński<sup>3</sup> · Krzysztof J. Kurzydłowski<sup>3</sup>

Submitted: 25 January 2018 / in revised form: 10 August 2018 / Published online: 5 September 2018  
© The Author(s) 2018

**Abstract** Ti-Al-based intermetallics are promising candidates as coating materials for thermal protection systems in aerospace vehicles; they can operate just below the temperatures where ceramics are commonly used, and their main advantage is the fact that they are lighter than most other alloys, such as MCrAlY. Therefore, Ti-Al-Si alloy coatings with five compositions were manufactured by spraying pure Ti and Al-12 wt.% Si powders using warm spray process. Two-stage hot pressing at 600 and 1000 °C was applied to the deposits in order to obtain titanium aluminide intermetallic phases. The microstructure, chemical composition, and phase composition of the as-deposited and hot-pressed coatings were investigated using SEM, EDS, and XRD. Applying of hot pressing enabled the formation of dense coatings with porosity around 0.5% and hard  $Ti_5(Si,Al)_3$  silicide precipitates. It was found that the  $Ti_5(Si,Al)_3$  silicides existed in two types of morphologies, i.e., as large particles connected together and as small isolated particles dispersed in the matrix. Furthermore, the produced coatings exhibited good isothermal and cyclic oxidation resistance at a temperature of 750 °C for 100 h.

**Keywords** applications, spray forming · feedstock, coatings for engine components · intermetallics · testing

## Introduction

Titanium aluminides are promising as a coating material, especially for thermal protection on Ti alloys (e.g., IMI 834) used under high-temperature and harsh environmental conditions in aerospace, automobile, and gas turbine industries because of their high specific strengths and excellent properties at elevated temperature (Ref 1-6). Industrial application of such coatings, however, is limited due to the complicated production routes. TiAl-based coatings might be fabricated by thermal spray techniques which can either use aluminide powder or deposits consisting of Ti and Al powder mixtures followed by heat treatment (Ref 7-10). However, there are some problems with production of coatings using Ti and Al powder mixture as a feedstock. In our previous study, pure Ti and Al powders were deposited by warm spray, which is a modification of high-velocity oxy-fuel (HVOF) spray process, also called as a two-stage HVOF, and Ti-Al phases were synthesized by two-stage heat treatment (Ref 10, 11). Accordingly, Ti-Al intermetallic phases were formed with a porosity up to 30% mostly due to the Kirkendall effect. It is generally known that Al is diffusing much faster than Ti which resulted in outflow of Al balanced by a large number of vacancies near the Al particles that condensed into pores during heat treatment. Pores increased in their volume due to the further formation of intermetallic phases, because of the difference in density between these phases and the elemental powders from which they form (Ref 12). Since dense microstructure of coatings is required for good mechanical properties as well as oxidation resistance at

✉ Judyta Sienkiewicz  
judyta.sienkiewicz@wat.edu.pl

<sup>1</sup> Institute of Armament Technology, Faculty of Mechatronics and Aerospace, Military University of Technology, Kaliskiego 2, 00-908 Warsaw, Poland

<sup>2</sup> National Institute for Materials Science, Research Center for Structural Materials, 1-2-1, Sengen, Tsukuba-Shi, Ibaraki-ken 305-0047, Japan

<sup>3</sup> Faculty of Materials Science and Engineering, Materials Design Division, Warsaw University of Technology, Woloska 141, 02-507 Warsaw, Poland

high temperatures, hot pressing was applied to coatings consisting of Ti and Al deposits (Ref 11). To obtain a dense microstructure, a pressure of 30 MPa was applied during the heat treatment leading to significant reduction in porosity to a range of around 5%, which still was too high.

Hence, it is of great interest to develop more effective fabrication methods for manufacturing of coatings based on TiAl phase, especially from elemental powders, that are relatively inexpensive and with good deformability compared to other intermetallic powders. Moreover, the addition of further alloying elements to the initial metal mixture is considered as it can affect both the fabrication of TiAl-based coatings and the properties of the final coatings. For instance, Si can improve not only the room temperature ductility, creep resistance, and high-temperature oxidation resistance, but it can also be expected to promote the densification process of coatings, which was also proved in our previous study (Ref 11). However, in order to obtain a dense coating, even with the addition of Si into the initial metal, heat treatment with applied pressure is required. Novak et al. reported the porosity of materials prepared by self-propagating high-temperature sintering from powder mixture of Ti and Al-30 wt.% Si alloy powders was still high (7 to 80 vol.% depends on the chemical composition) mostly due to the gas evolution from volatile impurities and changes in molar volume during reaction (Ref 13).

In this study, warm spray technique (WS) was used to produce the initial coatings. In WS, nitrogen gas is mixed with a supersonic combustion gas jet (Ref 14). Thanks to this system, the temperature of the propellant gas can be effectively controlled so that the temperature of the sprayed particle can be kept below its melting point. It can take advantage of thermal softening of the materials to lower the velocity needed to form bonding while avoiding excessive oxidation by keeping the particle temperature under the melting point, especially when it is applied to Ti and its alloys (Ref 15–17).

The main objective of this work was to develop an oxidation-resistant Ti-Al-based coatings that could be used as coating material for thermal protection systems. Titanium-aluminum-silicon coatings with five different chemical compositions were fabricated by warm spraying. In order to convert the deposits of Ti and Al-Si powder particles into the TiAl intermetallic phases, two-stage heat treatment under the pressure of 30 MPa was carried out. Attempts were made to reduce the porosity and improve the microstructure of the coatings, which is essential to obtain oxidation-resistant coatings for Ti alloys. Therefore, the oxidation resistance of the produced coatings was studied at 750 °C up to 100 h.

## Experimental

The experimental powder mixtures were prepared from commercially available Ti powder (TILOP -45 µm, Sumimoto, Tokyo, Japan) and Al-12 at.% Si alloy (Amdry 355, Oerlikon Metco, Tokyo, Japan). The Ti and Al-Si powder mixtures with five different chemical compositions (as listed in Table 1) were prepared as a feedstock for warm spraying. Figure 1 shows SEM image of the powder mixture PM 3 consisting of Ti and Al-12 at.% Si particles.

All powder mixtures were mixed mechanically for 3 h and deposited on stainless steel (SUS 316L) substrates with dimensions of 50 × 50 × 5 mm by WS under the spraying conditions shown in Table 2. Grit blasting and degreasing were conducted just before spraying. Alumina grit size was around 425–500 µm and the blasting pressure was 0.5 MPa. Time for ultrasonic degreasing in acetone was 10 min.

For hot pressing, the coated specimens were cut into 10 × 26 mm pieces. Samples were heated at a heating rate of 10 °C/min and annealed at 600 °C for 8 h during the first stage and at 1000 °C for 6 h during the second stage. All the samples were furnace-cooled at an average rate of 1 °C/min. The hot pressing was conducted in argon atmosphere, while the uniaxial stress of 30 MPa was applied during the first and second stage of heat treatment. In this process, heat was produced within the mold when it was subjected to a high-frequency electromagnetic field, generated by using an induction coil coupled to an electronic power supply; the mold was made of graphite and pressure was applied by one cylinder. After hot pressing, the samples prepared from powder mixtures PM 3 and PM 4 were encapsulated in evacuated quartz tubes and underwent homogenizing heat treatment in an electric furnace at 1000 °C for 100 h.

Obtained coatings were sectioned, mounted in epoxy resin, and metallographically polished before cross section observation. Scanning electron microscopy (JEOL, JSM-6010) with an acceleration voltage at 20 kV was performed on the surfaces and cross sections of the samples to study the microstructure of the feedstock powder, and as-sprayed and hot-pressed deposits. Phase analyses were performed

**Table 1** Composition of the experimental powder mixtures

Powder mixture no.	Ti, at.%	Al, at.%	Si, at.%
PM 1	37.0	55.5	7.5
PM 2	42.0	51.0	7.0
PM 3	46.8	47.0	6.2
PM 4	57.0	38.0	5.0
PM 5	67.0	29.0	4.0

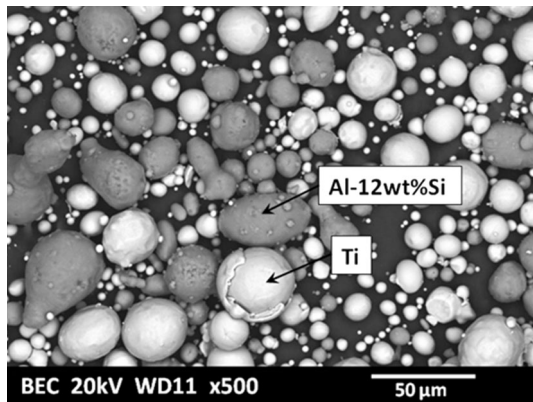


**Fig. 1** SEM (secondary electron mode) image of the powder mixture PM 3 (Ref 10)

**Table 2** Warm spray conditions

Kerosene flow rate	0.303 dm <sup>3</sup> /min
Oxygen flow rate	0.623 m <sup>3</sup> /min
Nitrogen flow rate	1.5 m <sup>3</sup> /min
Barrel length	200 mm
Spray distance	200 mm
Powder feed rate	16 g/min
Spray gun traversing velocity	700 mm/sec
Gun traverse pitch	4 mm

by x-ray diffraction (Rigaku Rint-2500 diffractometer) using Cu K<sub>α</sub> radiation for an angle range ( $2\theta$ ) of 20–80° with a step of 0.02° and scan speed of 1° per minute.

Porosity and coating thickness were evaluated by image analysis (Image J, National Institute of Health) performed on SEM cross section images. For the measurement of porosity, ten images were captured in the backscattered electron mode from each sample at 500 magnification and analyzed to calculate the average value. Microhardness tests were performed on the cross sections with 0.5 kgf loading with 10 measured points.

A heat flux-type DSC apparatus (NETZSCH 3300S) was used for analysis of the temperature-induced process taking place during the hot pressing of warm sprayed coatings. Samples used for these experiments were weighted about 20 mg and were placed in an alumina crucible with a diameter of 3 mm. The DSC experiments were carried out at a heating rate of 6 °C/min up to 1000 °C and followed by “natural” cooling in the DSC chamber. An argon flow of 50 ml/min was used in order to suppress sample oxidation.

Coatings for oxidation test were sprayed by using PM 3 and PM 4 powders on disks with a diameter of 20 mm made of a Ti alloy—IMI 834, hot-pressed, and homogenized. Isothermal and cyclic oxidation tests were carried out on coatings at 750 °C up to 100 h and 100 cycles,

respectively, using an electric furnace. One thermal cycle consisted of heating for 1 h at 750 °C and cooling in the ambient air atmosphere for 40 min. Each specimen was placed in a crucible, and all crucibles were placed on a platform, around which an electrical furnace repeated the horizontal motion, i.e., after 1 h heating in the furnace, it slides out on a rail to expose the samples to the ambient air. The surface of the oxidized samples was Ni-plated to prevent damage on the oxide scale during the sample’s cutting and polishing.

## Results and Discussion

### Microstructure of As-Sprayed and Heat-Treated Coatings

Representative cross-sectional secondary electron (SE) images of the as-sprayed coatings prepared from powder mixtures PM 1–PM 5 are shown in Fig. 2. These coatings consist of highly deformed aluminum-silicon “matrix” with hardly distinguishable particle boundaries, into which relatively undeformed Ti particles were embedded (Ref 10, 11). Al underwent much more deformation than Ti because of its lower yield strength and much lower melting point.

The characteristics of the as-sprayed coatings prepared from powder mixtures PM 1–PM 5 are given in Table 3. The thickness of sprayed coatings varied from 176 to 430 μm, whereas the average total porosity was generally in the range of 2–10 vol.% and occurred only in the Al-Si matrix, see Table 3. The difference in the coatings’ thickness indicates that the powder mixtures with higher Ti contents had higher deposition efficiency. In Table 3, the theoretical and obtained areas of Ti are also included. The analyses obtained from the SEM pictures show a loss of Ti particles during the spraying process for powder mixtures PM 1–PM 3 which is due to the difference in the melting point and specific heat between Ti and Al-12 at.% Si. However, for coatings prepared from powder mixtures PM 4 and PM 5 increased and close to theoretical amounts of Ti particles were observed.

Due to the relatively low temperature during WS, no aluminum or titanium oxides were detected by XRD in the as-sprayed deposits, which was confirmed in our previous studies (Ref 10, 11).

Representative SEM images of the hot-pressed coatings produced from powder mixtures PM 3 and PM 4 are shown in Fig. 3, which reveal fully dense coatings where only small pores were detected with the measured porosity of less than 0.5%. During the hot pressing, Ti reacted with Al-12 at.% Si and resulted in the formation of homogenized microstructures consisting of intermetallic phases with fine

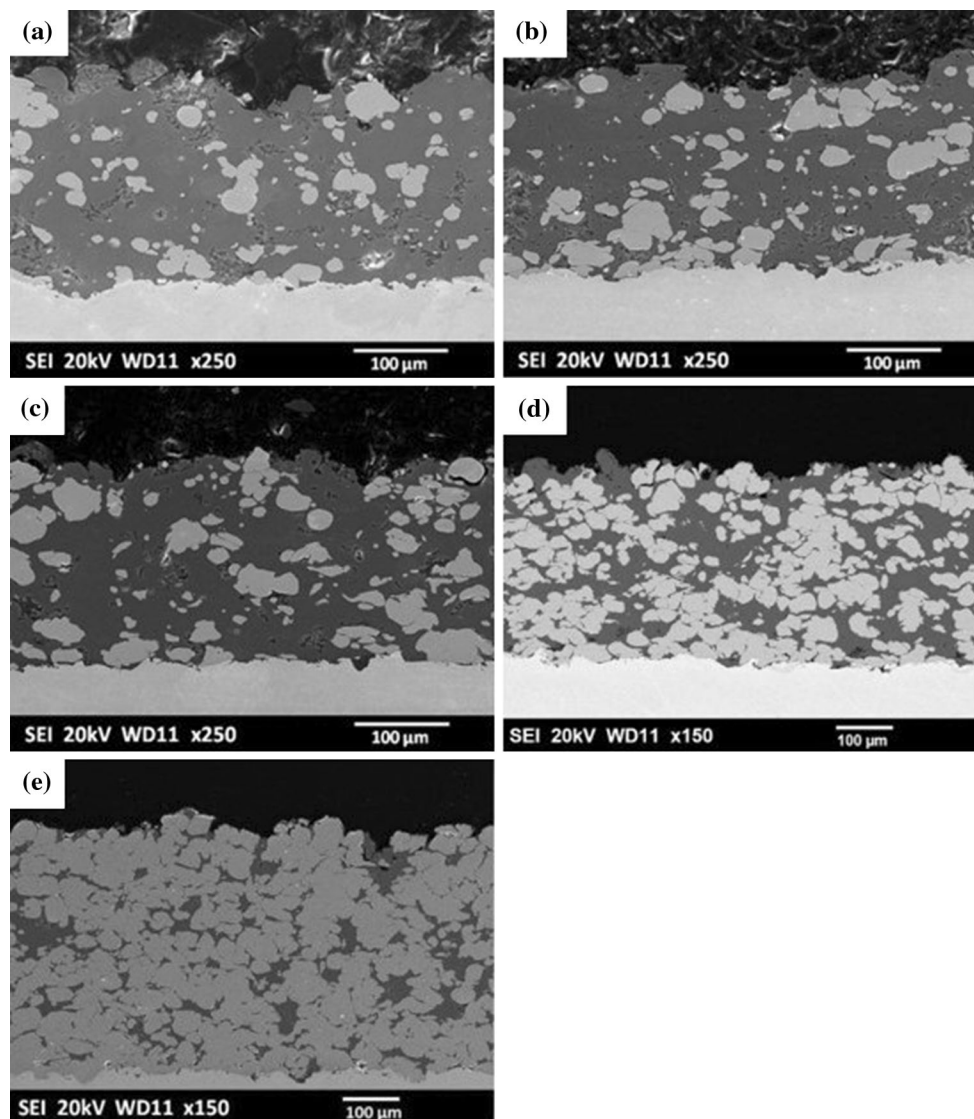


**Fig. 2** SEM (secondary electron mode) images of cross sections of as-sprayed coatings made from powder mixtures (a) PM 1, (b) PM 2, (c) PM 3, (d) PM 4, (e) PM 5 by warm spray (Ref 10)

**Table 3** Characteristic of the as-sprayed coatings

	PM 1	PM 2	PM 3	PM 4	PM 5
Coating thickness, $\mu\text{m}$	$176 \pm 8$	$193 \pm 10$	$192 \pm 9$	$300 \pm 12$	$430 \pm 15$
Porosity, %	10	8	5	2	2
Area occupied by Ti, %	23	36	35	55	78
Theoretical area occupied by Ti, %	42	46	52	54	68

irregularly shaped and randomly distributed silicides, see Fig. 3 and Table 4.

A higher-magnification cross section of Fig. 3(a) shown in Fig. 4(a) reveals that the microstructure is composed of large numbers of small particles (A) and some blocks of particles (B) distributed in the matrix. The blocks are actually clusters of small particles. The precipitations are arranged in the shapes similar to the shape of Ti powder

particles which were observed in the coatings in the as-sprayed state. The formation of many titanium silicides on the surfaces of Ti particles can be connected with two factors (a) the fact that Al-Si diffuses much faster than Ti and (b) with the fast reactivity between Ti and Si.

EDS point analysis (Fig. 4) and XRD patterns (Fig. 5) show formations of intermetallic phases after hot pressing. In all the coatings both Ti-Al intermetallic phases as well

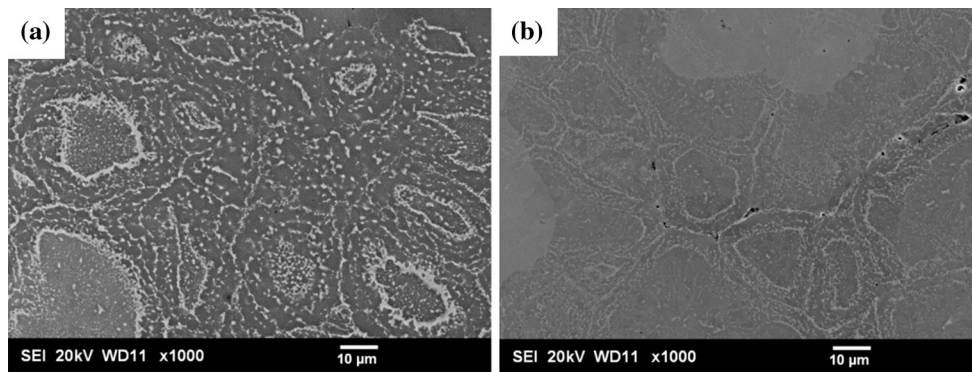
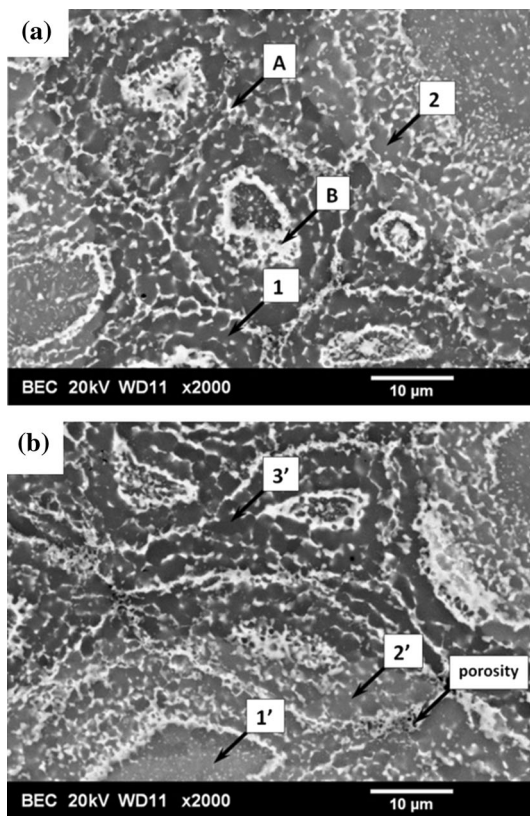


**Fig. 3** SEM images of cross sections of hot-pressed coatings made from powder mixtures: (a) PM 3, (b) PM 4 by warm spray



	1	2	1'	2'	3'
Ti[at.-%]	38	50	71	53	39
Al[at.-%]	60	49	26	40	58
Si[at.-%]	2	1	3	7	3

**Fig. 4** SEM image (backscatter mode) showing the titanium silicide precipitation and EDS point analysis in hot-pressed coatings from powder mixture (a) PM 3, (b) PM 4

as titanium silicide precipitation are present. Addition of Si to Ti-Al matrix resulted in the formation of titanium silicides since the solubility of Si in Ti-Al intermetallic phases is limited to 2.3, 0.8, and 13.6 at.% for  $Ti_3Al$ ,  $TiAl$ , and  $TiAl_3$ , respectively (Ref 18, 19). As shown in Fig. 4 and 5

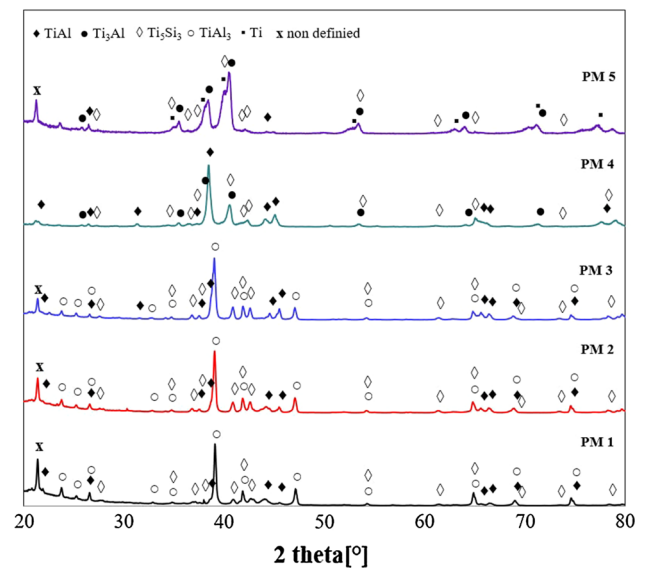


**Fig. 5** XRD patterns for hot-pressed coatings made from PM 1-PM 5 by warm spray

for coatings made from powder mixtures PM 1-PM 3, the microstructure is composed mostly of areas rich in Al which correspond to  $TiAl_3$  as well as areas which correspond to  $TiAl$  intermetallic phase. Moreover, there are a large number of precipitations which correspond to  $Ti_5Si_3$  silicides. The coating made from powder mixture PM 4 consists of three intermetallic phases, which can be denoted as  $TiAl_3$ ,  $TiAl$ , and  $Ti_3Al$ , and  $Ti_5Si_3$  silicides are also present. XRD analysis shows that the microstructure of coating made from powder mixture PM 5 is composed of regions which correspond to  $TiAl$  and  $Ti_3Al$  intermetallic phases and areas rich in Ti (> 90% of Ti) as well as a minute amount of  $Ti_5Si_3$  silicides. It was observed that this coating reacted with the substrate significantly; therefore, areas rich in Fe were observed (proved by XRD on samples where steel as a substrate material was used; not shown here). It can be associated with the presence of a large

amount of Ti particles which can easily react with the steel substrate.

On the basis of the SEM pictures, the areas occupied by each phase were calculated. Due to high specific strengths and excellent high-temperature properties, TiAl intermetallic phase is the most desirable phase from the Ti-Al equilibrium system. The highest content of this phase was obtained for the coatings produced from the powder mixtures with Ti/Al/Si ratio of 46.8:47.0:6.2 and 57.0:38.0:5.0. Moreover, in regard to the addition of secondary particles to the alloy matrix, the most important feature is chemical and mechanical compatibility between the matrix and reinforcement.  $Ti_5Si_3$  has been considered to be an effective phase to improve the properties of TiAl alloys as it possesses high strength and what is extremely important its thermal expansion coefficient is close to TiAl (Ref 20, 21).

To promote the formation of TiAl intermetallic phase, homogenizing heat treatment at 1000 °C for 100 h was carried out for coatings fabricated with powder mixtures PM 3 and PM 4. Representative SEM images of the coatings after additional heat treatment at 1000 °C are shown in Fig. 6.

It is clearly shown in Fig. 6 that the microstructure of coatings after the additional heat treatment is more homogenous than the microstructure of the only hot-pressed coatings. Coatings without homogenizing heat treatment were composed of TiAl,  $TiAl_3$ , and  $Ti_3Al$  intermetallics, whereas coatings after homogenizing heat treatment consisted mostly of TiAl phase which was proved by XRD measurement (Fig. 7). Nevertheless, it can be noticed that quite large amount of  $Ti_3Al$  phase was detected for coating produced from PM 4. Hence, it can be stated that annealing is more favorable for the coating PM 3 mainly due to the higher TiAl intermetallic phase content. Moreover, a large number of precipitations corresponding to  $Ti_5Si_3$  silicides were observed for both coatings.

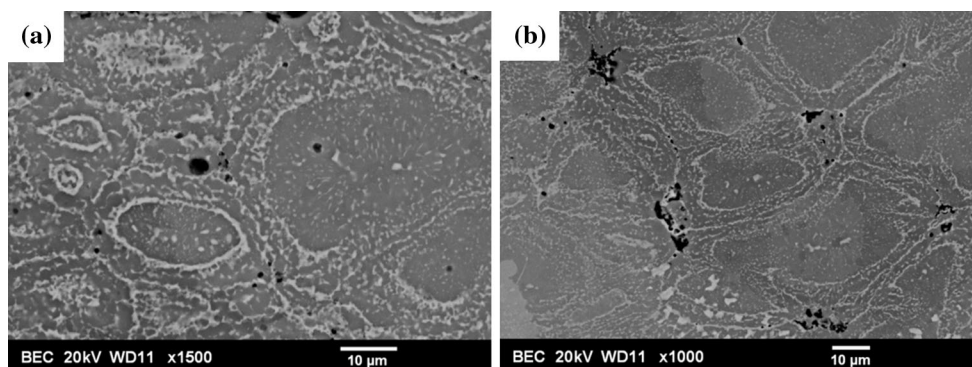


**Fig. 6** Backscattered electron images of hot-pressed coatings after heat treatment at 1000 °C for 100 h made from powder mixtures (a) PM 3, (b) PM 4

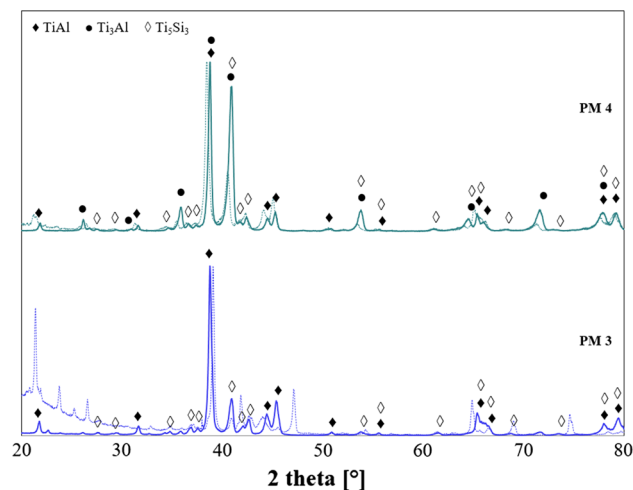


**Fig. 7** XRD patterns (solid lines) for hot-pressed coatings with additional heat treatment made from PM 3 and PM 4; dashed lines correspond to XRD patterns for hot-pressed coatings made from PM 3 and PM 4 by warm spray (the patterns of the hot-pressed PM 3 and PM 4 samples were repeated to appreciate the differences more clearly)

A slight increase in porosity (up to 1%) was also observed in all coatings subjected to additional heat treatment. It is associated with the formation of new phases (especially TiAl phase) and with the different density of the newly formed phases. Porosity is mostly observed in places where  $TiAl_3$  was and arisen mainly due to the fact that the newly formed TiAl intermetallic phase is denser than  $TiAl_3$ .

### Hardness Results

The Vickers microhardness values of hot-pressed coatings were  $620 \pm 10$  and  $450 \pm 8$  HV for the coatings prepared from powder mixtures PM 3 and PM 4, respectively. The higher hardness value of PM 3 coating is related to the existence of a greater amount of  $TiAl_3$ , which has the

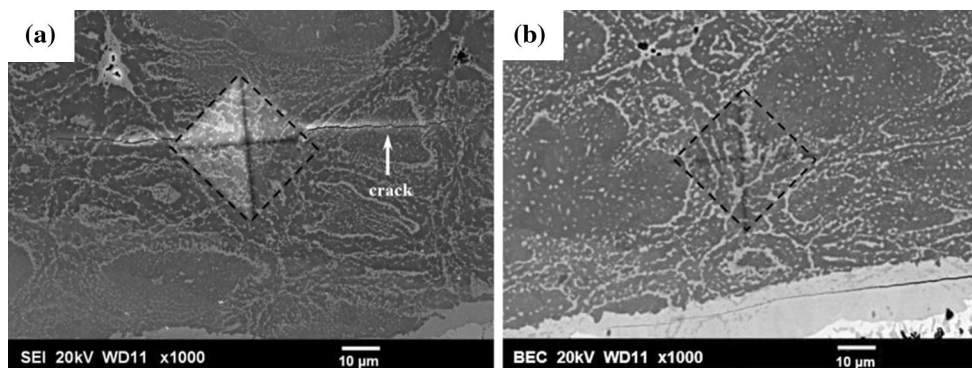


**Fig. 8** SEM image of typical indentation marks done on (a) hot-pressed coating prepared from powder mixture PM 3 and (b) hot-pressed coating with additional heat treatment at 1000 °C for 100 h prepared from powder mixture PM 3

highest hardness among Ti–Al intermetallic phases. A large number of cracks, however, were found around indentation marks for this coating (Fig. 8a). Some cracks were also observed for the coating made from PM 4. Cracks were mostly in the  $\text{TiAl}_3$ -formed intermetallic phase areas (proved by EDS analysis), which should be related to the fairly high brittleness of this phase.

Typical indentation marks for samples after homogenizing heat treatment at 1000 °C for 100 h are shown in Fig. 8(b) (indentation marks for the sample prepared from PM 4 were not shown here). In Fig. 8(b), the indentation mark is located on the border between TiAl and  $\text{Ti}_3\text{Al}$  phases. Furthermore, the pyramid indentations for both coatings are decidedly greater than the small  $\text{Ti}_5\text{Si}_3$  particles distributed in the matrix. The microhardness values were  $550 \pm 12$  and  $440 \pm 9$  HV for the heat-treated coatings made from powder mixtures PM 3 and PM 4, respectively. The microhardness value is lower for heat-treated coatings than it is for only hot-pressed coatings due to the elimination of the brittle  $\text{TiAl}_3$  phase. Moreover, for these coatings after additional heat treatment, no cracks were found around any of the several indentation marks made during Vickers hardness test also because of the elimination of the  $\text{TiAl}_3$  phase.

### DSC Results

Figure 9 shows DSC curves for the coating produced from powder mixture PM 3 as well as a coating produced from Ti and Al powder mixture with Ti/Al ratio of 50:50 (used in our previous study (Ref 11)). For the coating produced from Ti and Al powder, there is an exothermic peak at 640 °C, which corresponds to the reaction between Ti and Al. No peak indicating the melting of Al was detected. The disappearance of the endothermic peak (which is usually observed for powder mixtures of Ti and Al and which corresponds to melting of Al) was caused by the generation

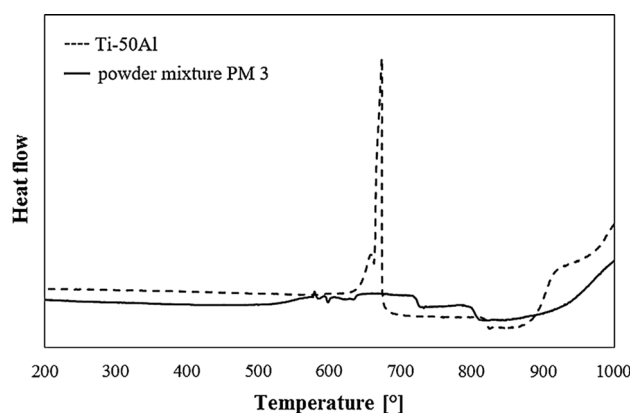


**Fig. 9** DSC curves for as-sprayed coatings prepared from powder mixture PM 3 and from Ti and Al powder mixture with Ti/Al ratio of 50:50

of large quantity of heat during the formation of  $\text{TiAl}_3$ , which is much higher than the heat required to melt Al. The large quantity of heat is emitted during this reaction because Ti and Al in coatings were very closely packed and diffusion, even in the solid state, was rapid. Altogether, the endothermic peak corresponding to the melting of Al in the present case is covered by the larger exothermic peak that corresponds to the reaction between Ti and Al occurring close to the melting point of Al.

It can be clearly seen that Si affects the reaction between Ti and Al. DSC lines show that Si addition influences the kinetics of the reaction between Ti and Al, specifically slowing down the reaction. The solid curve reveals several perceivable locations where phase reactions and changes occur. The reactions which can occur during heating are related mostly to the formation of titanium silicides. The significantly smaller thermal effect that occurs between Ti and Al–Si eutectic alloy than in binary Ti–Al suggests that Si affects the mechanism of the reaction of Al with Ti. The

reaction between Si and Ti has more negative Gibbs energy than the reaction of Al with Ti, and therefore  $Ti_5Si_3$  silicide is the easiest to form, so it would be formed primarily. Moreover, the reaction that occurs between Ti and Si is exothermic, so the heat could generate enough high temperature to obtain liquid metal enabling to fill the pores. After both Ti + Si and Ti + Al reactions have finished, the material becomes completely solid (Ref 12).

The most important difference between the Ti and Al-Si system and Ti-Al phase diagram is the generation of the eutectic Al-Si liquid at 570 °C in the ternary mixture foreseen by the phase diagram. Replacement of pure Al by eutectic Al-Si alloy can lead to densification process of coatings due to the fact that Al-Si eutectic liquid possesses better fluidity than Al liquid and hence its ability to fill the gaps between more solid Ti particles is much better (Ref 11).

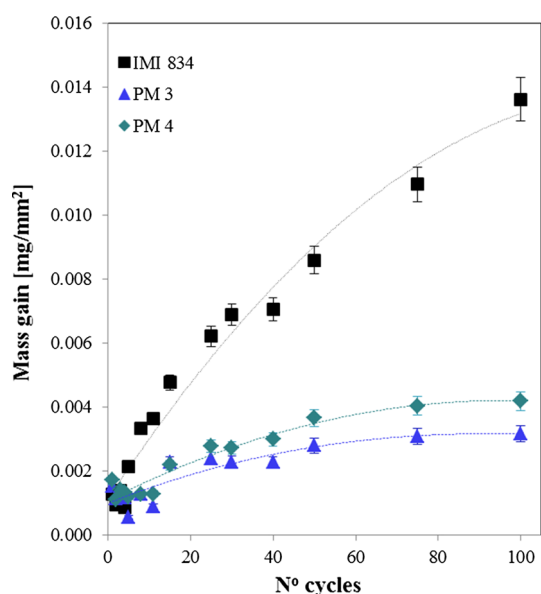


**Fig. 10** Specific weight variations during cyclic oxidation of uncoated and Ti-Al-Si-coated specimens of IMI 834

## Isothermal and Cyclic Oxidation Test

The measured weight gains per unit surface area of the annealed base IMI 834 alloy, as well as those with Ti-Al-Si coatings made from PM 3 and PM 4 mixture after isothermal oxidation test at 750 °C for 100 h, were 0.0253, 0.0108, and 0.0037  $mg\ mm^{-2}$ , respectively. It can be pointed out that the Ti-Al-Si coatings reduced weight gain during the oxidation test in comparison with the bare IMI 834.

Figure 10 compares the mass gain curves of the uncoated and coated IMI 834 specimens during thermal cyclic oxidation at 750 °C for 100 h. As can be noted, the mass gain rate for both the bare and coated IMI 834 alloy was faster at the beginning of the oxidation test. A stable oxide scale that covers the entire surface is formed after about 25 h at this temperature for both coatings. After that period, the mass gain rate for the coated IMI 834 decreased greatly, while the mass gain rate for bare IMI 834 still remained quite high. The total mass gain for IMI 834 was 0.013, whereas for coatings with the addition of Si it is 0.00316 and 0.00418  $mg\ mm^{-2}$ , respectively, for the coatings made from PM 3 and PM 4. This result indicated that the coatings decreased the cyclic oxidation rate of the IMI 834 alloy significantly.

Surface morphology of Ti-Al-Si coatings after isothermal oxidation treatment is shown in Fig. 11(a) and (b). The SEM observation indicates that the surface morphology of oxide scales differs for different coatings, which is related to the chemical and phase compositions. Nevertheless, a uniform oxide layer was formed on Ti-Al-Si coating consisting mostly of  $TiO_2$ . However, some  $Al_2O_3$  particles were observed on the surface. It is believed that the large oxide particles are  $TiO_2$  and the small oxide grains are  $Al_2O_3$  by EDS results and by considering their respective growth rates— $TiO_2$  grows much faster than  $Al_2O_3$ . The surface morphologies of the oxide scale after cyclic oxidation testing at 750 °C lasting 100 h, on the coatings made from PM 3 and PM 4, are presented in Fig. 11(c) and (d). Based on the EDS measurement (that is not shown here), it can be concluded that the outer layer of the scale is composed mostly of  $TiO_2$  oxide with some  $Al_2O_3$  crystals. For the coating made from PM 4, acicular small-sized

**Table 4** Area occupied by each phase in hot-pressed coatings

Powder mixture	TiAl <sub>3</sub>	Ti-Al (TiAl)	Ti <sub>3</sub> Al	> 90% of Ti	Phase rich in Fe	Silicides (Ti <sub>5</sub> Si <sub>3</sub> )	Porosity
PM 1	55	27	...	...	...	18	0.5
PM 2	39	45	...	...	...	16	0.5
PM 3	29	56	...	...	...	14	0.5
PM 4	7	61	23	...	...	9	0.5
PM 5	...	10	40	30	12	8	0.5



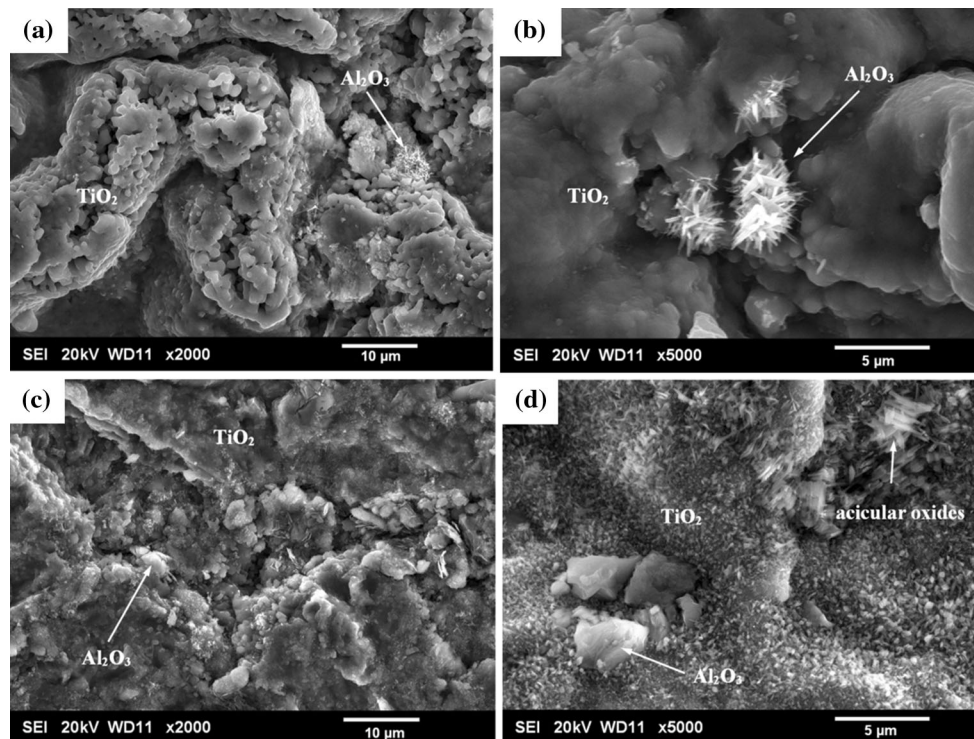


**Fig. 11** Surface morphology of Ti-A-Si coatings after isothermal oxidation test at 750 °C for 100 h in air made from (a) PM 3, (b) PM 4 and after cyclic oxidation test at 750 °C by 100 cycles in air made from (c) PM 3, (d) PM 4

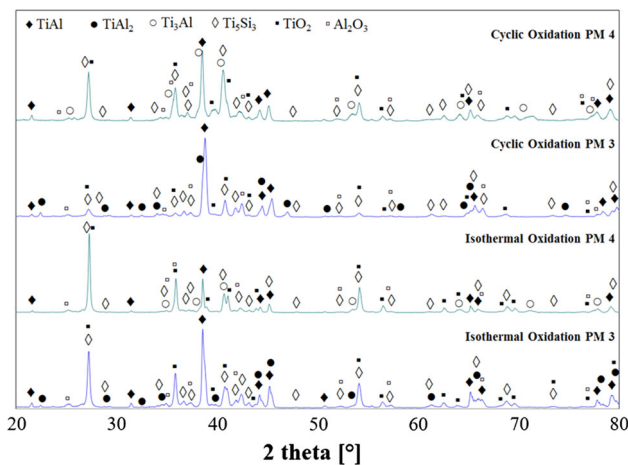


**Fig. 12** XRD patterns for the Ti-Al-Si coatings after isothermal and cyclic oxidation test at 750 °C for 100 h in air made from PM 3 and PM 4

oxides are observed. It is believed that these oxides correspond also to  $Al_2O_3$ .

XRD measurement results proved that oxide scales after isothermal and cyclic oxidation test consist of  $TiO_2$  (rutile) and  $Al_2O_3$  (alpha-alumina), see Fig. 12.  $TiAl$  and  $Ti_5Si_3$ , which are the main phases of the coating material, show the strongest peaks, indicating that very thin scale was formed

even after the long-term oxidation at 750 °C. Peaks from  $TiAl_2$  phase for coatings prepared from powder mixture PM 3 were also detected. Some nitrides such as  $TiN$  were also observed, whereas no Si oxides were detected which indicates that silicon was dissolved in titanium and aluminum oxides.

Figure 13 shows the backscattered electron micrographs of cross sections of the oxidation layer formed on the two Ti-Al-Si coatings. In both cases, the oxide layers with a thickness of  $\sim 1 \mu m$  are continuous and well adherent to the coatings. It should be pointed out from Fig. 12 and 13, as the amount of Si addition increases, the oxidation scale becomes thinner and the oxides formed on the alloys become finer and smoother. For the coating from PM 3, some cracks were detected in the isothermally and cyclic oxidized samples, see Fig. 14.  $TiO_2$  oxides in shape of coarse crystals are formed onto the coatings on precipitations of  $Ti_5Si_3$  phase. Initiation of cracking in the oxidation layer as well as spallation of the oxides may be related both to the fact that  $TiO_2$  grows much faster than  $Al_2O_3$  and to the brittleness of the  $Ti_5Si_3$  phase—it is clearly seen on the cross sections of oxides layers in Fig. 13. Moreover, cracks through coatings can be related to a non-uniformity of the structure, which results in thermal stresses (inducted by a difference of coefficient of thermal expansion CTE).

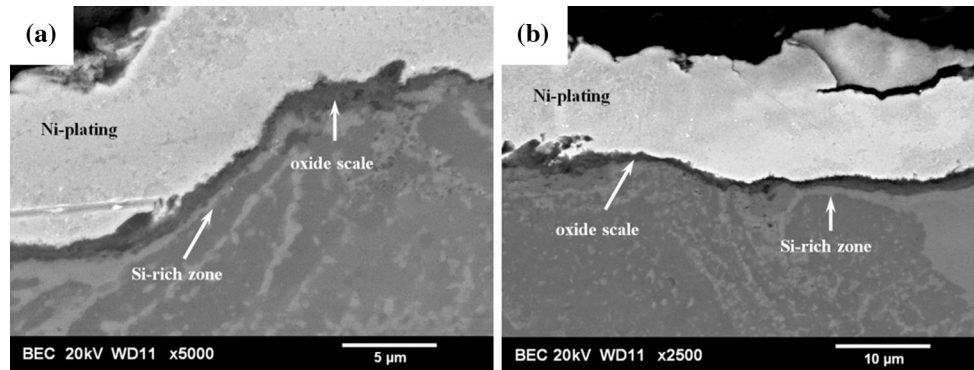


**Fig. 13** SEM images of cross sections of scales formed on Ti-Al-Si coatings after cyclic oxidation test at 750 °C for 100 h in air made from (a) PM 3, (b) PM 4

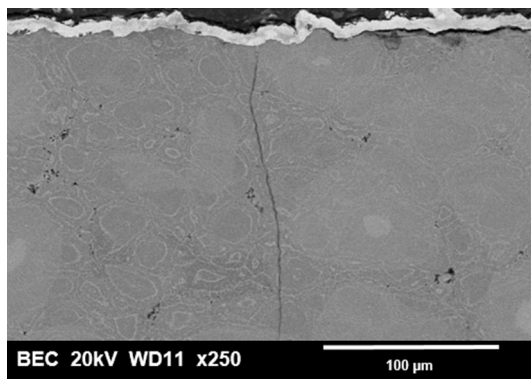


**Fig. 14** SEM image of the cross section of Ti-Al-Si coating made from PM 3 after cyclic oxidation test at 750 °C for 100 h in air

It can be concluded from the literature survey that the Si addition changes the microstructure of the oxidation scale on TiAl-based alloys (Ref 22, 23). Although the  $\text{SiO}_2$  scale is not formed because of the low content of Si in thermally sprayed coatings, the addition of Si is beneficial to the oxidation resistance. Si has good affinity with Ti so that they can form titanium silicides as  $\text{TiSi}_2$ ,  $\text{Ti}_5\text{Si}_3$ ,  $\text{Ti}_5\text{Si}_4$ , and  $\text{TiSi}$  that exhibit high oxidation resistance (Ref 22).

Precipitations of  $\text{Ti}_5\text{Si}_3$  that occur in both PM 3 and PM 4 coatings are stable enough to endure long-term high-temperature oxidation. Si reduces the mobility of Ti because the latter is bound to form stable compounds. Considering that the Si-rich layer beneath the oxide scale was continuous and compact, it could serve not only as outward diffusion barrier for Ti but also as inward diffusion barrier for oxygen (Ref 23). Consequently, the degradation rate of the diffused coating has been lowered, which could prolong its life.

Furthermore, the poor oxidation resistance of TiAl alloy at high temperatures results from the outward diffusion of Ti and inward diffusion of oxygen. However, with the addition of Si, the fine dense film can be formed on the surface of the TiAl-based alloy. The oxidation scale is composed of alternated  $\text{TiO}_2$  and  $\text{Al}_2\text{O}_3$  layers, where the  $\text{Al}_2\text{O}_3$  layer is dense and the outer layer of the scale contains  $\text{TiO}_2$ . The inner layer is formed by inward diffusion of oxygen ions and the outer layer by outward diffusion of metal ions (Ref 24, 25). Formation of the  $\text{Al}_2\text{O}_3$ -rich layer beneath titania can be explained by the fact that Si stabilizes Ti and enhances the thermodynamic activity of Al. The same arguments explain the existence of Si-rich zone (mostly composed of  $\text{Ti}_5\text{Si}_3$ ) on the oxide/coating

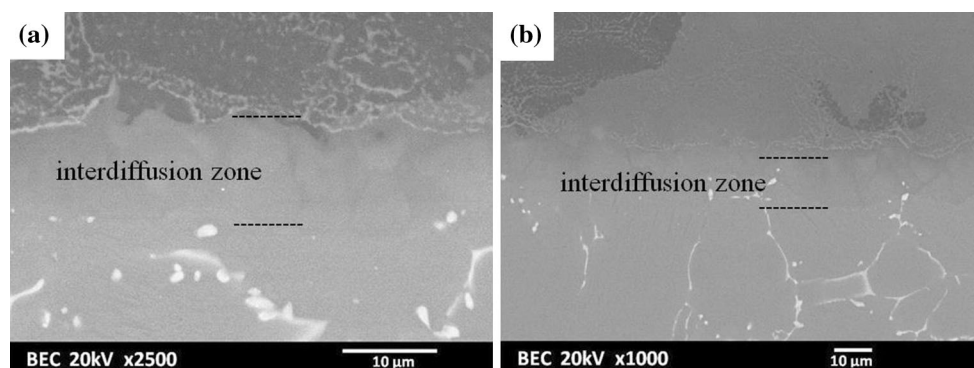


**Fig. 15** SEM images of interdiffusion layers between the substrate and Ti-Al-Si coatings after cyclic oxidation test made from (a) PM 3, (b) PM 4

interface. Due to the low solid solubility of Si in the oxidation scale, as the oxidation scale grows, Si gathers in the diffusion zone, which enhances the activity of Al further leading to locating the Al<sub>2</sub>O<sub>3</sub>-rich layer always on the interior side of the oxidation scale. Moreover, when the Si content exceeds a certain value a uniformly dense Al<sub>2</sub>O<sub>3</sub> layer will form on the interior side of oxidation scale (Ref 25). Xiao et al. (Ref 26) showed that dense and protective Al<sub>2</sub>O<sub>3</sub> layer forms at the early stage of oxidation process.

It is worth to note that the interdiffusion zones between the substrate and the Ti-Al-Si coatings after oxidation test were very thin, see Fig. 15. For both types of coatings, the thickness of such interdiffusion zones which were enriched in Al was below 10 μm.

## Conclusions

Ti-Al matrix coatings reinforced with titanium silicide precipitates were fabricated by heat treatment of hot-pressed coatings prepared by warm spraying of Ti and Al-12 at.% Si powders.

The obtained coatings mainly consisted of:

- TiAl, TiAl<sub>3</sub>, and fine precipitates of titanium silicide for coatings prepared from powder mixtures with the Ti/Al ratio of 60:40, 55:45, and 50:50;
- TiAl, Ti<sub>3</sub>Al, and Ti<sub>5</sub>Al<sub>3</sub> precipitates for coatings prepared from powder mixtures with the Ti/Al ratio of 60:40 and 70:30.

Homogenizing heat treatment was performed on the hot-pressed coatings made of the powder mixtures with Ti/Al/Si ratio of 46.8:47.0:6.2 and 57.0:38.0:5.0, which led to the formation of coatings with more homogenous microstructure with low porosity consisting mostly of TiAl intermetallics with Ti<sub>5</sub>Si<sub>3</sub> precipitates. It was found that Ti<sub>5</sub>Si<sub>3</sub> existed in two types of morphologies, i.e., as large particles connected together forming a netlike structure and as small isolated particles dispersed in the matrix. It was noticed that the coatings after additional heat treatment were less brittle as no cracks were generated near indentation marks during Vickers microhardness measurement.

The results show also that the addition of Si decreased the reaction between Ti and Al and was beneficial to densification process of the TiAl intermetallic coatings.

The Ti-Al-Si coatings obtained from the powder mixtures with the Ti/Al ratio of 50:50 and 60:40, after additional homogenization, exhibited excellent resistance to isothermal and cyclic oxidation at 750 °C during 100 h because Si addition to the coatings resulted in a compact Al<sub>2</sub>O<sub>3</sub> layer in the oxidation scale.

**Acknowledgments** The authors are grateful to Mr. T. Hiraoka for operating the thermal spray equipment. The results presented in this paper have been obtained during Ph.D. studies at Warsaw University of Technology, Faculty of Materials Science and Engineering, Division of Materials Design under WUT-NIMS Joint Graduate Program.

**Open Access** This article is distributed under the terms of the Creative Commons Attribution 4.0 International License (<http://creativecommons.org/licenses/by/4.0/>), which permits unrestricted use, distribution, and reproduction in any medium, provided you give appropriate credit to the original author(s) and the source, provide a link to the Creative Commons license, and indicate if changes were made.

## References

1. T. Noda, Application of Cast Gamma TiAl for Automobiles, *Intermetallics*, 1998, **6**, p 709-713
2. T. Tetsui, Development of a TiAl Turbocharger for Passenger Vehicles, *Mater. Sci. Eng., A*, 2002, **329-331**, p 582-588
3. B.P. Bewlay, M. Weimer, T. Kelly, and A. Suzuki, The Science, Technology and Implementation of TiAl Alloys in Commercial Aircraft Engines, *2012 MRS Fall Meet.*, 2012.
4. S.L. Draper, D. Krause, B. Lerch, I.E. Locci, B. Doehnert, R. Nigam, G. Das, P. Sickles, B. Tabernig, N. Reger, and K. Rissbacher, Development and Evaluation of TiAl Sheet Structures for Hypersonic Applications, *Mater. Sci. Eng., A*, 2007, **464**, p 330-342
5. G.P. Chaudhari and V.L. Acoff, Titanium Aluminide Sheets Made Using Roll Bonding and Annealing Reaction, *Intermetallics*, 2010, **18**, p 472-478
6. F. Appel and R. Wagner, Microstructure and Deformation of Two-Phase γ-Titanium Aluminides. *Mater. Sci. Eng.* 187-268 (1998)
7. T. Sasaki, T. Yagi, T. Watanabe, and A. Yanagisawa, Aluminizing of TiAl-Based Alloy Using Thermal Spray Coating, *Surf. Coatings Technol.*, 2011, **205**(13-14), p 3900-3904
8. T. Novoselova, P. Fox, R. Morgan, and W.O. Neill, Experimental Study of Titanium/Aluminium Deposits Produced by Cold Gas Dynamic Spray, *Surf. Coatings Technol.*, 2006, **200**, p 2775-2783
9. T. Novoselova, S. Celotto, R. Morgan, P. Fox, and W.O. Neill, Formation of TiAl Intermetallics by Heat Treatment of Cold-Sprayed Precursor Deposits, *J. Alloys Compd.*, 2007, **436**, p 69-77
10. J. Sienkiewicz, S. Kuroda, R.M. Molak, and H. Murakami, Fabrication of TiAl Intermetallic Phases by Heat Treatment of Warm Sprayed Metal Precursors, *Intermetallics*, 2014, **49**, p 57-64
11. J. Sienkiewicz, S. Kuroda, K. Minagawa, H. Murakami, and H. Araki, Effects of Al Content and Addition of Third Element on Fabrication of Ti-Al Intermetallic Coatings by Heat Treatment, *J. Therm. Spray Technol.*, 2015, **24**(5), p 749-757
12. R.W. Rice and W.J. McDonough, Intrinsic Volume Changes of Self-Propagating Synthesis, *J. Am. Ceram. Soc.*, 1985, **68**(5), p 122-123
13. P. Novák, A. Michalcová, J. Šerák, D. Vojtěch, T. Fabián, S. Randáková, F. Průša, V. Knotek, and M. Novák, Preparation of Ti-Al-Si Alloys by Reactive Sintering, *J. Alloys Compd.*, 2009, **470**, p 123-126
14. S. Kuroda, J. Kawakita, M. Watanabe, and H. Katanoda, Warm Spraying—a Novel Coating Process Based on High-Velocity Impact of Solid Particles. *Sci. Technol. Adv. Mater.* **9**, (2008)
15. J. Kawakita, H. Katanoda, M. Watanabe, K. Yokoyama, and S. Kuroda, Warm Spraying: An Improved Spray Process to

- Deposit Novel Coatings, *Surf Coat Technol.* 4369-4373 (2008)
16. R.M. Molak, H. Araki, M. Watanabe, H. Katanoda, N. Ohno, and S. Kuroda, Warm Spray Forming of Ti-6Al-4V, *J. Therm. Spray Technol.*, 2014, **23**(1-2), p 197-206
  17. S. Kuroda, R.M. Molak, M. Watanabe, and H. Araki, Velocity Measurement of Sprayed Particles and Coatings Fabrication of Titanium Alloys by High-Pressure Warm Spray. *Therm. Spray 2013 Proc. Int. Spray Conf.* **6**, 263-265 (2013)
  18. S. Tsuyama, S. Mitao, and K. Minakawa, Alloy Modification of  $\gamma$ -Base Titanium Aluminide for Improved Oxidation Resistance, Creep Strength and Fracture Toughness, *Mater. Sci. Eng., A*, 1992, **153**, p 451
  19. F.-S. Sun and F.H. Sam, Froes, Precipitation of silicide Phase in TiAl Alloys, *Mater. Sci. Eng., A*, 2002, **A328**, p 113-121
  20. O.N. Senkov, M. Cavusoglu, and F.H. Froes, Synthesis and Characterization of a TiAl-Ti5Si3 Composite with a Submicrocrystalline Structure, *Mater. Sci. Eng. A*, 2001, **A300**, p 85-93
  21. R. Gerling, A. Bartels, H. Clemens, M. Oehring, and F.-P. Schimansky, Properties of Two-Phase Intermetallic (Ti, Nb)<sub>3</sub>(Al, Si) + (Ti, Nb)<sub>5</sub>(Si, Al)<sub>3</sub> P/M Bulk and Sheet Material, *Acta Mater.*, 1997, **45**, p 4057-4066
  22. M. Goral, L. Swadzba, G. Moskal, M. Hetmanczyk, and T. Tetsui, Si-Modified Aluminide Coatings Deposited on Ti46Al7Nb Alloy by Slurry Method, *Intermetallics*, 2009, **17**(11), p 965-967
  23. J. Wang, L. Kong, J. Wu, T. Li, and T. Xiong, Microstructure Evolution and Oxidation Resistance of Silicon-Aluminizing Coating on  $\gamma$ -TiAl Alloy, *Appl. Surf. Sci.*, 2015, **356**, p 827-836
  24. S. Taniguchi, H. Juso, and T. Shibata, Improvement in High-Temperature Oxidation Resistance of TiAl by Addition of 0.2 Mass% Zr, *Mater. Trans.*, 1996, **37**(3), p 245-251
  25. H.R. Jiang, Z.L. Wang, W.S. Ma, X.R. Feng, Z.Q. Dong, L. Zhang, and Y. Liu, Effects of Nb and Si on High Temperature Oxidation of TiAl, *Trans. Nonferrous Met. Soc. China*, 2008, **18**, p 512-517
  26. W. Xiao, L. Zhang, and H. Jian, Effects of Si on High Temperature Oxidation Resistance of TiAl Alloy, *J. Beijing Univ. Aeronaut. Astronaut.*, 2006, **32**, p 365-368